# The crystal structure of sphingosine-1-phosphate in complex with a Fab fragment reveals metal bridging of an antibody and its antigen

Jonathan M. Wojciak[a,1], Norman Zhu[b,1], Karen T. Schuerenberg[b], Kelli Moreno[a], William S. Shestowsky[a], Masao Hiraiwa[a], Roger Sabbadini[a], and Tom Huxford[b,2]

[a]LPath Inc., 6335 Ferris Square, Suite A, San Diego, CA 92121; and [b]Structural Biochemistry Laboratory, Department of Chemistry and Biochemistry, San Diego State University, 5500 Campanile Drive, San Diego, CA 92182-1030

Edited by Gregory A. Petsko, Brandeis University, Waltham, MA, and approved August 31, 2009 (received for review June 4, 2009)

**The pleiotropic signaling lipid sphingosine-1-phosphate (S1P) plays significant roles in angiogenesis, heart disease, and cancer. LT1009 (also known as sonepcizumab) is a humanized monoclonal antibody that binds S1P with high affinity and specificity. Because the antibody is currently in clinical trials, it is important to confirm by structural and biochemical analyses that it binds its target in a predictable manner. Therefore, we determined the structure of a complex between the LT1009 antibody Fab fragment and S1P refined to 1.90 Å resolution. The antibody employs unique and diverse strategies to recognize its antigen. Two metal ions bridge complementarity determining regions from the antibody light chain and S1P. The coordination geometry, inductively coupled plasma spectroscopy, surface plasmon resonance spectroscopy, and biochemical assays suggest that these are $Ca^{2+}$. The amino alcohol head group of the sphingosine backbone is recognized through hydrogen bonding interactions from 1 aa side chain and polypeptide backbone atoms of the antibody light and heavy chains. The S1P hydrophobic tail is almost completely enclosed within a hydrophobic channel formed primarily by the heavy chain. Both treatment of the complex with metal chelators and mutation of amino acids in the light chain that coordinate the metal atoms or directly contact the polar head group abrogate binding, while mutations within the hydrophobic cavity also decrease S1P binding affinity. The structure suggests mechanistic details for recognition of a signaling lipid by a therapeutic antibody candidate. Moreover, this study provides direct structural evidence that antibodies are capable of using metals to bridge antigen:antibody complexes.**

antibody structure | calcium | lipid signaling | x-ray crystallography

Sphingolipids are primary structural components of cell membranes that also serve as cellular signaling and regulatory molecules (1). The sphingolipid signaling cascade, of which ceramide (CER), sphingosine (SPH), and sphingosine-1-phosphate (S1P) are the most widely studied components, has recently become appreciated for its roles in the cardiovascular system, angiogenesis, and tumor biology (2). The sphingolipid signaling molecule S1P (Fig. 1*A*) is produced from SPH through the action of sphingosine kinase. While CER and SPH are commonly associated with apoptosis, S1P is a mediator of cell proliferation and an activator of survival pathways (3–5). S1P functions as an extracellular mediator of cell survival that can activate a set of G Protein-Coupled Receptors belonging to the S1P/LPA receptor family, formerly known as Edg receptors (6). However, intracellular signaling roles for S1P have also been suggested (7).

In an effort to design therapeutics that target biologically active lipids, we have produced a monoclonal antibody that specifically binds the S1P tumor growth factor in the physiological concentration range and is capable of neutralizing its effects in vivo (8, 9). A fully humanized form of the antibody, which we refer to here as LT1009 (also known as sonepcizumab), has been developed and is currently in Phase 1 trials for cancer as the systemic formulation named ASONEP while an ocular formulation known as iSONEP is in Phase 1 clinical trials for Age-Related Macular Degeneration (AMD). To better understand the molecular determinants for S1P binding specificity, we have determined the x-ray crystal structure of the Fab fragment of LT1009 in complex with S1P. The complex structure reveals a mechanism for the specific binding of a biologically active small molecule lipid by an antibody.

## Results

**Structure Determination.** LT1009 (sonepcizumab) was generated by grafting the CDR loops of the murine parent antibody (Sphingomab) onto a human IgG1K isotype framework (Fig. 1*B*). Several residues in the framework of the variable domain were mutated back to the murine sequence to restore high affinity S1P binding (9). Standard methods were used for large-scale whole antibody generation, purification, papain proteolysis, and Fab purification. Complexes suitable for crystallization were formed by incubating the Fab and S1P in an aqueous emulsion followed by filtration. Initial $2F_O - F_C$ map building with reflection intensities measured to a minimum Bragg spacing of 2.70 Å and phases derived from molecular replacement yielded a clear extra electron density within the suspected antigen binding site. After fitting and refining the atoms of S1P, 2 spheres of electron density that were visible when contoured at 5.0 $\sigma$ remained unaccounted for. On the basis of local *B*-factors, coordination geometry, ligand chemistry, bond lengths, and resulting difference maps the 2 sites were assigned as $Ca^{2+}$ ions. This assignment was made despite the fact that the same coordination observed in the S1P:LT1009 Fab complex is also preferred by $Mg^{2+}$ and the crystal formed in 100 mM $MgSO_4$. The x-ray structure was subsequently refined against diffraction data collected to 1.90 Å (Table 1).

**Overall Complex Structure.** The LT1009 antibody heavy and light chains are numbered according to the system of Kabat and Wu (10). The LT1009 Fab fragment structure exhibits the standard Ig domain folds (Fig. 2*A*). Interest in the structure of the LT1009 Fab derives from its high affinity binding of the bioactive lipid S1P and the direct participation of a pair of $Ca^{2+}$ ions in S1P

Author contributions: J.M.W., N.Z., M.H., R.S., and T.H. designed research; J.M.W., N.Z., K.T.S., K.M., W.S.S., and T.H. performed research; J.M.W., N.Z., and T.H. contributed new reagents/analytic tools; J.M.W., N.Z., and T.H. analyzed data; and J.M.W. and T.H. wrote the paper.

The authors declare no conflict of interest.

This article is a PNAS Direct Submission.

Data deposition: The atomic coordinates have been deposited in the Protein Data Bank, www.pdb.org (PDB ID code 3I9G).

[1]J.M.W. and N.Z. contributed equally to this work.

[2]To whom correspondence should be addressed. E-mail: thuxford@sciences.sdsu.edu.

This article contains supporting information online at www.pnas.org/cgi/content/full/0906153106/DCSupplemental.

BIOCHEMISTRY

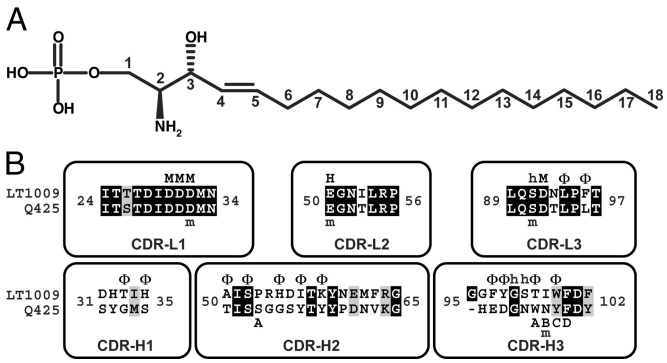


**Fig. 1.** Schematic representations of S1P and LT1009. (*A*) The structure of S1P in its uncharged form with stereochemistry and numbering of the carbon atoms indicated. (*B*) The primary amino acid sequence of the CDRs from the LT1009 heavy and light chains is shown in single letter code. Numbering is according to Kabat and Wu convention with letters A–D below indicating insertions. For comparison, the CDR sequences from the anti-CD4 Q425 antibody are aligned and identical and homologous residues are indicated by black and light gray boxes, respectively. Residues directly involved in S1P binding are indicated by the following letters above the sequence: M-binds $Ca^{2+}$; H-hydrogen bonds through a side chain; h-hydrogen bonds through peptide backbone atoms; Φ-mediates hydrophobic interactions. Amino acids that were observed to contact $Ca^{2+}$ in the Q425 Fab x-ray structure are indicated by the letter ''m'' below.

binding (Fig. 2*B*). This is the first example of which we are aware wherein metal ions are directly observed in a crystal structure to bridge an antibody and its epitope.

The antibody-bound S1P adopts a slightly curled conformation as it perfectly fits the refined electron density with near ideal stereochemistry, bond lengths, and angles (Fig. 2*B*). Other than the presence of the 2 bridging metal ions, the most striking feature of the S1P:LT1009 Fab complex structure is the extent to which the ligand is almost completely engulfed by its antibody (Fig. 2*C*). In its antibody-bound conformation, S1P measures approximately 407 $Å^2$ of total molecular surface area (11). Upon binding to the antibody, 276 $Å^2$ of the S1P molecular surface becomes buried. This places S1P among the group of higher than average buried surface percentage as a function of molecular surface area when compared to other antibody-bound nonpeptide small molecules (12). The exposed surfaces of S1P include the greater portion of the phosphate head group and the terminal carbon atom. The latter served as the point of attachment when the S1P hapten was prepared synthetically for immunization (9). Thus, the LT1009 Fab intimately contacts nearly all atoms in S1P, consistent with its relatively small size and high-affinity of interaction.

**Inductively Coupled Plasma (ICP) Spectroscopy.** To confirm the identity of the bound metal ions, the same purified, concentrated S1P:LT1009 Fab complexes used for crystallization were analyzed by ICP spectroscopy. When measured against Hepes buffer and calibrated with dilute solutions of $Ca^{2+}$, $Mg^{2+}$, and $Mn^{2+}$ salts in pure water, the only metal detected at levels >50 ppb in the samples was $Ca^{2+}$. Comparison against the total protein complex concentration yielded a ratio of ≈2 $Ca^{2+}$ ions per complex. The fact that $Ca^{2+}$ is present within these complexes at all is surprising, because $Ca^{2+}$ was not intentionally introduced during any of the multiple chromatographic, dialysis, and concentration steps. Although the lipid used in these studies is synthetic and supplied as a zwitterionic salt without counterions, ICP analysis of the S1P:methanol emulsion used for complex formation revealed that it also contained detectable levels of $Ca^{2+}$ (1–2 μM). Interestingly, when either unbound LT1009 whole IgG or Fab fragments were analyzed by ICP, the amount of detected $Ca^{2+}$ corresponded to approximately one metal ion per antigen binding site.

**Table 1. Data collection and refinement statistics**

| | S1P:LT1009 Fab |
|---|---|
| *Data collection* | |
| X-ray source | ALS 5.0.1 |
| Wavelength (Å) | 0.97741 |
| Space group | $P2_12_12_1$ |
| Unit cell (Å) | |
| a | 66.052 |
| b | 70.889 |
| c | 138.719 |
| Complexes/asymmetric unit | 1 |
| Resolution range[a] | 50.0–1.90 (1.99–1.90) |
| $R_{sym}$ (%) | 5.5 (40.1) |
| Observations | 255,775 |
| Unique reflections | 50,494 |
| Completeness (%) | 97.0 (76.8) |
| Redundancy | 5.1 (3.3) |
| $<I/\sigma>$ | 26.4 (2.2) |
| *Refinement* | |
| $R_{cryst}$ (%) | 19.0 (25.7) |
| $R_{free}$ (%)[b] | 21.9 (27.6) |
| Protein atoms | 3,361 |
| Ligand/Metal/Solvent atoms | 25/7/283 |
| R.m.s.d. | |
| Bond lengths (Å) | 0.013 |
| Bond angles (°) | 1.542 |
| Mean *B* factors($Å^2$) | |
| Protein atoms | 27.5 |
| S1P | 27.1 |
| Calcium | 30.7 |
| Magnesium | 56.6 |
| Solvent | 35.7 |
| Ramachandran plot[c] | |
| Favored | 96.5% |
| Allowed | 3.3% |
| Disallowed | 0.2% |
| PDB accession code | 3I9G |

[a]Data in parentheses are for highest resolution shell.
[b]Calculated against a cross-validation set of 5.1% of data selected at random prior to refinement.
[c]Calculated from MOLPROBITY (15)

**Metal Binding.** The 2 bound $Ca^{2+}$ occupy neighboring sites in the S1P:LT1009 Fab complex crystal structure (Fig. 3*A*). Their coordination sphere is created both by amino acid side chains from the LT1009 light chain and the phosphate group of S1P. Both $Ca^{2+}$ ions are octahedrally coordinated through one terminal *syn* $\eta^1$ bond from either AspL31 to Ca1 or AspL92 to Ca2 (throughout this paper the letters "L" and "H" immediately before amino acid numbers indicates that they derive from light or heavy chains, respectively). Two bridging $\mu$-$\eta^1$:$\eta^1$ interactions with AspL30 and AspL32 side chains provide another pair of bonds to each metal ion. Two separate pairs of water molecules occupy symmetrically similar positions about the ions thus providing 2 additional coordinating oxygen atoms to the complex. Finally, an oxygen atom from the phosphate head group of S1P completes the coordination of both ions with a $\mu$ bridge. This ligand arrangement allows the 2 $Ca^{2+}$ to come within 3.8 Å of one another without any linking atoms directly between them. The coordination chemistry of this complex is similar to that observed in nucleic acid-bound type II restriction endonucleases such as BamHI and PvuII, which require $Mg^{2+}$ for activity and are inhibited by $Ca^{2+}$ (13, 14).

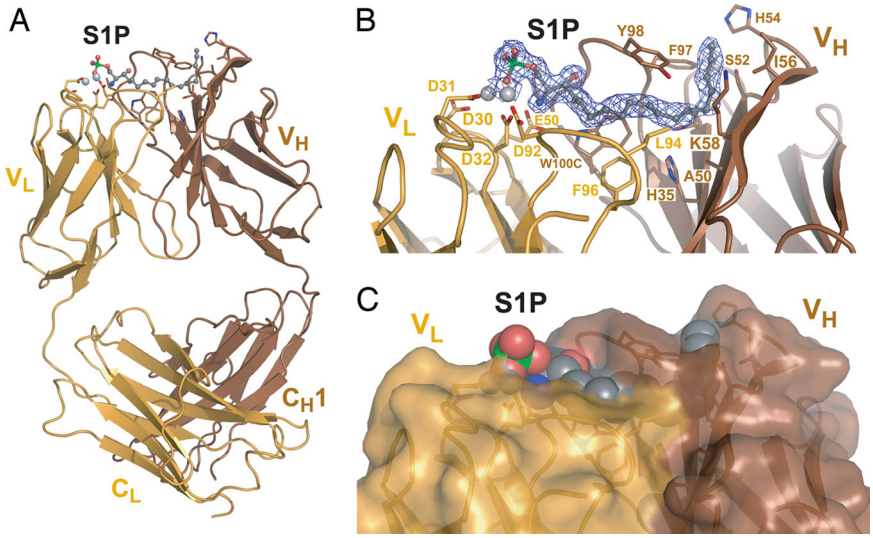


**Fig. 2.** X-ray crystal structure of the LT1009 Fab:S1P complex. (*A*) A ribbon diagram representation of the antibody Fab fragment. The light chain is colored gold and the heavy chain is brown. S1P is depicted as a ball-and-stick model with cpk coloring and the 2 $Ca^{2+}$ ions are represented as light gray spheres. (*B*) Close-up view of the S1P binding site. Electron density from a 2 $F_O$ - $F_C$ refined map contoured at 1.1 $\sigma$ is displayed for the region of the model within 1.9 Å of each atom in S1P. (*C*) A semitransparent surface representation of the Fab reveals the extent to which S1P, represented as cpk spheres, is buried upon binding to LT1009.

To test the importance of metal binding to complex formation, we measured the apparent affinity of whole IgG LT1009 antibody for S1P by ELISA in the presence of increasing concentrations of chelators (Fig. 3*B*). This experiment revealed that S1P binding can be completely inhibited by the addition of either EDTA or the $Ca^{2+}$-selective chelator EGTA at concentrations >10 $\mu$M. When full-length LT1009 was first preincubated with 50 $\mu$M EDTA or EGTA, S1P binding could be restored by the addition of either $Mg^{2+}$ or $Ca^{2+}$ (Fig. 3*C*). $Mg^{2+}$ rescued S1P binding at significantly lower concentrations in the EGTA-treated antibody. These results suggest that both $Mg^{2+}$ and $Ca^{2+}$ are capable of bridging the LT1009 antibody and the phosphate on its S1P epitope and further illustrate the extremely stable binding of $Ca^{2+}$ in the complex cocrystals.

In an effort to assign a gain of function role for divalent metals in the S1P:LT1009 interaction, we compared LT1009 Fab binding affinity to an immobilized S1P derivative by surface plasmon resonance (SPR) spectroscopy in the presence and absence of $Ca^{2+}$. By this analysis, the LT1009 Fab binds S1P with an apparent equilibrium dissociation binding constant ($K_D$) of 130 ± 30 nM ($n$ = 3). Supplementing the buffer with 50 $\mu$M $CaCl_2$ increased the apparent affinity to 1.1 ± 0.1 nM ($n$ = 3) (Fig. 3*D*). Both the association and dissociation rate constants shift toward a higher affinity interaction in the presence of $Ca^{2+}$ (Table 2). While it is likely that the presentation of S1P covalently attached to a 2D surface leads to the differences observed when comparing values of binding affinity measured by SPR to those in solution, the >100-fold increase in affinity is consistent with the crystal structure and chelation studies in demonstrating that $Ca^{2+}$ plays a major role in S1P:LT1009 complex formation.

**Antigen Binding.** Affinity and specificity in LT1009 binding of S1P derives from a series of complementary noncovalent interactions with the lipid (Fig. 4). The first of these is an electrostatic attraction between the 2 bound $Ca^{2+}$ and a single oxygen atom from the phosphate head group (Fig. 4*A*). Considering that the antibody contributes only 3 bonds to each of the bound $Ca^{2+}$ and in light of their proximity to one another, we suspect that $Ca^{2+}$ does not occupy these sites in the absence of bound S1P (see *Discussion*).

The second set of interactions involves direct contacts be-

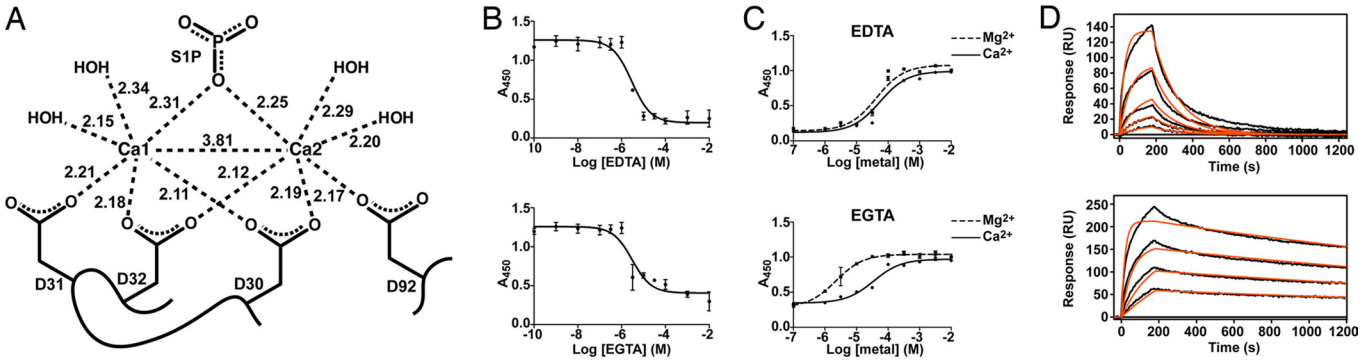


**Fig. 3.** Bridging $Ca^{2+}$ ions are required for S1P binding by LT1009. (*A*) Schematic diagram of $Ca^{2+}$ coordination with bond lengths in Å and LT1009 light chain amino acids labeled. (*B*) Incubation of full length LT1009 with increasing concentrations of either EDTA (*Top*) or EGTA (*Bottom*) inhibits S1P binding by ELISA. (*C*) Reintroduction of increasing amounts of either $Mg^{2+}$ or $Ca^{2+}$ to LT1009 antibodies preincubated with EDTA (*Top*) or EGTA (*Bottom*) restores the antibody's ability to bind S1P. (*D*) SPR sensorgrams of titrated LT1009 Fab binding to surface-bound S1P in the absence (*Top*) and presence (*Bottom*) of 50 $\mu$M $CaCl_2$. Raw measurements are plotted in black while curves that best fit the data are overlayed in orange.

**Table 2. Surface plasmon resonance spectroscopy of S1P:LT1009 Fab binding**

| | $k_a$ | $k_d$ | $K_D$ |
|---|---|---|---|
| | ($\times 10^4$ $M^{-1}s^{-1}$) | ($\times 10^{-4}$ $s^{-1}$) | (nM) |
| No $CaCl_2$ | 5.5 ($\pm$ 0.8) | 70 ($\pm$ 7) | 130 ($\pm$ 30) |
| 50 $\mu$M $CaCl_2$ | 26 ($\pm$ 5) | 2.9 ($\pm$ 0.1) | 1.1 ($\pm$ 0.1) |

tween LT1009 and the amino alcohol region of S1P (Fig. 4*B*). Both the C2-amino and C3-hydroxyl groups of S1P participate in hydrogen bonding interactions. However, only the hydrogen bond between the carboxylic acid group of GluL50 and the amino group of S1P involves an amino acid side chain, suggesting that this interaction is critical for S1P specificity. The C3-hydroxyl moiety forms hydrogen bonds with the backbone amides of GlyH99 and SerH100, both from CDR-H3. S1P contains a *trans* double bond between carbons 4 and 5 (Fig. 1*A*). There is nothing observed in the crystal structure to suggest that this chemical group is specifically recognized. Consequently, it is not surprising that sphinganine-1-phosphate, the reduced dihydro version of the ligand, binds indistinguishably to the LT1009 antibody (9).

The remaining contacts between S1P and the LT1009 Fab are primarily hydrophobic in nature (Fig. 4*C*). Amino acids involved in these interactions include residues LeuL94 and PheL96 from the light chain and ThrH33, HisH35, AlaH50, SerH52, HisH54, IleH56, LysH58, PheH97, TyrH98, ThrH100A, and TrpH100C from the antibody heavy chain. Although several of these amino acids contain polar or charged side chains, each contribute to a network of closely packed carbon atoms and create a hydrophobic channel that surrounds the lipid aliphatic tail. For example, LysH58 runs the hydrophobic portion of its side chain parallel with the lipid tail and then projects its $\varepsilon$-amino group into the surrounding solvent. And HisH35 participates in 2 hydrogen bonds so that its $\varepsilon$-carbon atom can seal the floor of this hydrophobic chamber. TyrH98 occupies a key position within CDR-H3. Upon binding to S1P this loop adopts a conformation that folds to cover the top of the lipid, with TyrH98 functioning like a restraint, passing over the bound S1P molecule and fastening to the side chains of LeuL94 and LysH58 through van der Waals forces.

**Site-Directed Mutagenesis.** To confirm and assess the extent of participation of the observed interactions in stabilizing S1P binding, we performed site-directed mutagenesis coupled with in vitro binding assays (Fig. 4*D*). Mutation of either AspL30 or AspL32 to Ala completely inhibited the ability of LT1009 to bind S1P. This is not surprising as both amino acids contribute significantly to $Ca^{2+}$ coordination. Another series of mutations were made to assess the contribution to S1P binding of residues that form the hydrophobic pocket. Mutation of TyrH98 to alanine resulted in a significant decrease in binding. HisH35Ala/Gln mutations introduced in the core of this hydrophobic channel only marginally decreased S1P binding affinity. Mutation of HisH35 to Glu, however, completely disrupted formation of the complex. These data suggest that hydrophobic interactions between the tail of S1P and the LT1009 heavy chain are necessary for high affinity S1P:LT1009 complex formation. Introduction of a charged residue might allow water or ions to reside within the channel and block binding.

The most interesting mutation tested was GluL50 to Ala. This mutation, designed to assess the extent to which the hydrogen bond to the C2-amino group influences S1P:LT1009 complex formation, completely abrogates S1P binding. Loss of this hydrogen bond could be expected to decrease binding affinity and, perhaps, even decrease selectivity for S1P over structurally

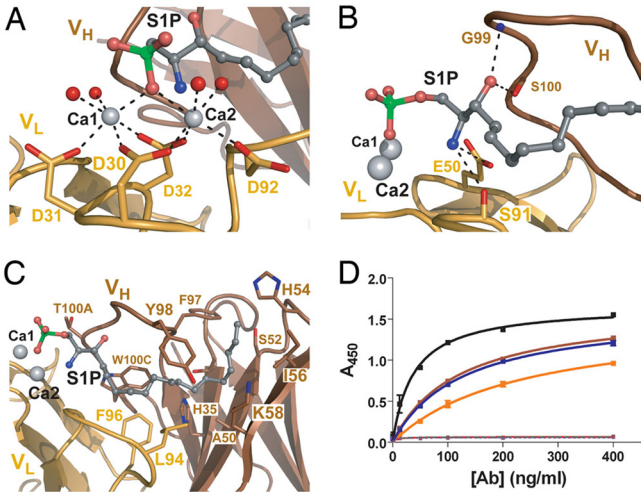


**Fig. 4.** A combination of noncovalent interactions mediate LT1009 binding to S1P. (*A*) The S1P phosphate group is indirectly contacted through a unique dual calcium bridging motif created by the antibody light chain. (*B*) The C2-amino and C3-hydroxyl groups of S1P participate in hydrogen bonds with both the antibody light and heavy chains. (*C*) Several amino acid side chains from both the antibody light and heavy chains participate in the formation of a hydrophobic channel that accommodates the aliphatic S1P tail. (*D*) Site-directed mutagenesis of residues at any of these positions affects S1P binding. Full length LT1009 binding to S1P by ELISA is depicted in black. Mutation of residues AspL30, AspL32, or GluL50 individually to alanines completely disrupts the ability of LT1009 to bind S1P (dashed red, green, and light blue lines, respectively). Likewise, mutation of HisH35 to glutamic acid completely blocks binding (purple dashed line). Mutation of HisH35 to either glutamine or alanine partially blocks binding as does replacement of TyrH98 with alanine (solid brown, blue, and orange lines, respectively).

related lipids. However, complete loss of S1P binding as a result of mutation of GluL50 suggests that this residue plays a larger role in the mechanism of S1P:LT1009 complex formation.

## Discussion

Our x-ray crystallographic and accompanying biochemical analyses confirm that the LT1009 antibody is capable of specific binding to the small bioactive lipid S1P. The challenge in selective binding of such targets becomes obvious when one considers that S1P contains only 25 nonhydrogen atoms and that 14 of them form a contiguous fully saturated linear hydrocarbon chain (Fig. 1*A*). LT1009 accomplishes this feat through a combination of electrostatic interactions, hydrogen bonds, and hydrophobic contacts that cover nearly 70% of the S1P molecular surface. Because typically there is a correlation between surface area and affinity, the S1P:LT1009 Fab complex crystal structure illustrates how the extremely efficient use of a minimum antibody surface area (CDR) can produce a high affinity interaction.

To recognize its epitope, the antibody employs a pair of bridging calcium ions. The critical role of $Ca^{2+}$ in stabilizing the S1P:LT1009 interaction is clearly demonstrated by the greater than 100-fold increase in apparent affinity when $Ca^{2+}$ is included in binding assays. The use of divalent ions is a strategy that has been used many times by enzymes and structural proteins. Some, such as the peripheral membrane protein annexin V, the C2 domain of protein kinase C$\alpha$, and Gla domain of human prothrombin, use $Ca^{2+}$ to bridge their interactions with phospholipids (15–17).

Antibodies have been observed previously to bind metals either as a consequence of their structure or as a result of their design (18, 19). In one recent study, the antibody Q425 was found to require $Ca^{2+}$ for high affinity binding to its antigen, the CD4

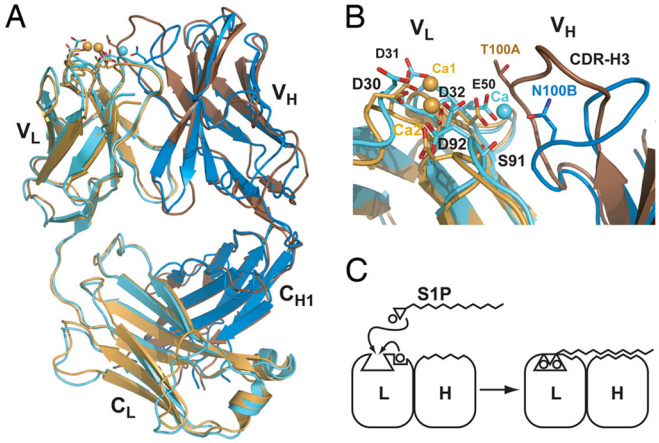


**Fig. 5.** (*A*) Overlay of LT1009 and Q425 anti-CD4 antibody Fab crystal structures illustrates their overall homology and different $Ca^{2+}$ binding sites. LT1009 is colored as in previous figures while the Q425 light chain is cyan and the heavy chain fragment is blue. For the sake of clarity, S1P has been removed from the LT1009 Fab model. (*B*) A close up view of $Ca^{2+}$ binding sites in the 2 models reveals conservation of metal coordinating side chains and the different conformations of CDR-H3. (*C*) Schematic representation of a possible mechanism of S1P binding by LT1009. In its unbound conformation, the light chain (labeled ''L'' in the figure) binds one $Ca^{2+}$ at a site similar to that observed in the Q425 antibody structures. S1P binding introduces conformational changes that disrupt the original $Ca^{2+}$ binding motif as well as potentially introducing one additional $Ca^{2+}$. The phosphate group of S1P then combines with 2 $Ca^{2+}$ to produce the extremely stable $Ca^{2+}$ coordination complex observed in the S1P:LT1009 Fab complex crystal structure.

receptor of helper T cells, in solution binding assays (20). The light chain CDR loops of the Q425 antibody display significant sequence homology to LT1009 including each of the 4 calcium coordinating aspartic acid residues as well as GluL50 (Fig. 1*B*). Interestingly, crystallographic analysis of the Q425 Fab either in the presence of $Ca^{2+}$ or with EDTA revealed that it binds to a single $Ca^{2+}$ at an alternative site. This is clearly illustrated when the $Ca^{2+}$:Q425 and S1P:LT1009 Fab complexes are superimposed (Fig. 5*A*). $Ca^{2+}$ in Q425 is coordinated through the side chains of AspL32, GluL50, and a backbone carbonyl oxygen from SerL91 on the light chain and AsnH100B from the heavy chain. All of these side chains occupy nearly identical positions as their counterparts in LT1009 with the exception of AsnH100B, which resides on the tip of CDR-H3 that displays a significant difference in conformation between the 2 structures (Fig. 5*B*). The binding affinity of Q425 for $Ca^{2+}$ was deduced by virtue of the effect of $Ca^{2+}$ on CD4:Q425 complex formation, suggesting that Q425 binds the metal in the 187 $\mu$M range. The variable domain antibody fragment MR1 is a third antibody with a nearly identical light chain sequence. X-ray crystallography of an MR1 Fv fragment revealed not only that it does not bind $Ca^{2+}$ but also that none of the potential light chain $Ca^{2+}$ coordinating amino acids are involved in contacting an EGFRvIII epitope peptide (21).

The structural observations made in these related antibodies combined with our structure, ICP, and mutagenesis data suggest that the 2 stably bound $Ca^{2+}$ we observe in the S1P:LT1009 Fab complex crystal structure do not likely occupy these sites in the absence of S1P. This raises questions as to the source of the 2 $Ca^{2+}$ ions. We speculate that antigen-free LT1009 contains one $Ca^{2+}$ bound at the alternative site observed in the $Ca^{2+}$:Q425 Fab structure (Fig. 5*C*). Upon S1P recognition, the CDR-H3 loop changes conformation and GluL50 from the light chain moves to hydrogen bond with the C2-amino group of S1P. These changes release the bound $Ca^{2+}$, which is immediately scavenged at the phosphate binding site. The remaining $Ca^{2+}$ might be associated with S1P. Our ability to detect $Ca^{2+}$ by ICP spectroscopy in the S1P emulsion used in our complex formation protocol supports this hypothesis. It remains to be seen whether $Ca^{2+}$ might similarly be associated with S1P in vivo as there is an abundance of $Ca^{2+}$ in extracellular fluid. This mechanism supports a fundamental role for GluL50 within the LT1009 light chain in providing a ''reservoir'' of $Ca^{2+}$ for complex formation during maturation and helps to explain why mutation of this residue is deleterious to ligand binding.

Besides satisfying the existing structural and biochemical observations, this model helps to explain why bridging metals have not been observed previously in antigen:antibody complex structures. Zhou et al. (20) suggest that to evolve interfacial metal binding the metal must ''bind to the Ab with sufficient affinity to comprise part of the recognition surface, but at the same time they must do so with only a partially filled coordination shell to permit additional ligation by antigen.'' This is likely true. However, in light of our observations it also seems reasonable that an alternative approach might be to couple relatively low affinity metal binding at one site with conformational change and high affinity antigen:metal:antibody complex formation. Experimental investigations into the kinetics of S1P binding by LT1009 and an antigen-free crystal structure will improve our understanding of this therapeutically relevant antibody.

## Materials and Methods

**Antibody Production and Fab Preparation.** Stable CD-CHO cells that produce LT1009 have been developed by Lpath as reported in a recent publication (9). Antibodies were purified by ProSep-vA-Ultra (Millipore) chromatography. LT1009 IgG was digested at a 100:1 ratio with activated papain (Worthington); the reaction was quenched with iodoacetamide, dialyzed, and purified by anion exchange chromatography. Fab-containing fractions were passed through a protein-A column, concentrated, and stored at 4 °C. A more detailed description of this and other experimental methods is available online as *SI Materials and Methods*.

**Complex Formation and Cocrystallization.** A 5-fold molar excess of 1 mM S1P (Avanti Polar Lipids) was resuspended in 500 $\mu$L of LT-1009 Fab (3.5 mg/mL), filtered, and concentrated to 12 mg/mL. Crystals were grown at room temperature by the hanging drop, vapor diffusion method. 1 $\mu$L of 12 mg/mL S1P:Fab complex was mixed with 1 $\mu$L of reservoir solution containing 22% (wt/vol) polyethylene glycol 3350, 100 mM $MgSO_4$, 100 mM Na citrate (pH 6.0), and 10% (vol/vol) ethylene glycol.

**Data Collection and Processing.** Home source x-ray diffraction data were collected at 100 K on an R-Axis IV++ image plate detector (Rigaku) and synchrotron data were collected on an ADSC 200 CCD detector at the Advanced Light Source Beamline 5.0.1 Berkeley National Laboratory. Data indexing and scaling were carried out by using HKL2000 (22). Data collection and refinement statistics are summarized in Table 1.

**Structure Solution, Model Building, and Refinement.** Molecular replacement was carried out in PHASER (23) and further refinement by maximum likelihood methods was run in REFMAC (24). The model was rebuilt in the program XTALVIEW (25). Coordinates for sphingosine-1-phosphate were prepared by adding a phosphate to sphingosine taken from the HIC-UP server (26). Stereochemical analysis and final adjustments to the model were directed by MOLPROBITY (27). Coordinates and structure factors were deposited to the Protein Data Bank (28). Figures were prepared in PyMOL (29).

**ICP Spectroscopy.** ICP analysis was carried out on a DV 4300 ICP Optical Emission Spectrometer (Perkin-Elmer Sciex). The instrument was calibrated with $CaCl_2$, $MgCl_2$, and $MnCl_2$ standards in water. The wavelengths used for detection of $Ca^{2+}$ were 315.891 nm and 317.933 nm; for $Mg^{2+}$ 279.553 nm, 280.271 nm, and 285.213 nm; and for $Mn^{2+}$ 257.61 nm. Intensity readings were measured in 10 × 2 second intervals and averaged (Table S1).

**Surface Plasmon Resonance Spectroscopy.** SPR experiments were performed on a BioRad ProteOn XPR36 system at 25 °C. An S1P derivative containing a thiol group at the C18 position was immobilized to a ProteOn GLM sensor chip using sulfo-MBS coupling to produce surface densities between 600 and 1200

BIOCHEMISTRY

RU. Binding experiments were carried out in the presence or absence of 50 $\mu$M $CaCl_2$. Data were double referenced by subtracting the responses from interstitial reference spots as well as blank injections using the analysis program Scrubber2-Pro (Biologic Software). Processed data were fit to a 1:1 interaction model to extract estimates of the binding constants.

**Site Directed Mutagenesis and Expression of Mutated Antibodies.** Plasmids harboring mutations within the variable domains of the heavy and light chains were prepared by using the QuikChange Site-Directed Mutagenesis Kit (Stratagene). Mutant plasmids were confirmed by DNA sequencing. Mutant LT1009 antibodies were produced from transiently transfected HEK 293F cells as described in ref. 9.

**Metal Chelation Studies.** Samples containing 150 ng/mL full length LT1009 and titrated with EDTA or EGTA (Boston Biosciences) were prepared in duplicate and analyzed by ELISA. To assay the effect of specific metal ion addition, samples containing 150 ng/mL full length LT1009 and either 50 $\mu$M EDTA or EGTA was titrated with $CaCl_2$ or $MgCl_2$ (Sigma). Each sample ($n = 2$) was evaluated in triplicate by S1P binding ELISA.

**S1P Binding ELISA.** Microtiter ELISA plates (Costar) were coated by incubation with S1P conjugated to delipidated BSA. Plates were washed and blocked before primary incubation of wild-type or mutant full length LT1009 antibodies. Plates were washed and incubated with HRP-conjugated goat anti-human IgG (Jackson Laboratory). After washing, peroxidase activity was measured with tetramethylbenzidine substrate (Sigma) and optical density (OD) was measured at 450 nm by using a Thermo Multiskan EX. Data were plotted by using Graphpad Prism software.

**ACKNOWLEDGMENTS.** We thank D. Myszka at Biosensor Tools, LLC for the SPR measurements, L. Thurn for access to ICP spectrometer, J.-J. Kim and R. J. Deschennes for invaluable contributions of equipment, B. Spingler, D. Sullivan, and N. Nguyen for overseeing assembly of the MXCF, and J.C. Ngo and F. Romesberg for critical discussion. The Advanced Light Source is supported by the Director, Office of Science, Office of Basic Energy Sciences, of the Department of Energy under Contract No. DE-AC02–05CH11231. Biochemistry research at San Diego State University is supported in part by the California Metabolic Research Foundation. T.H. is the recipient of an American Cancer Society grant RSG-08–287-01-GMC. Lpath, Inc. received partial support for this work through a phase 1 SBIR grant (1 R43 GM 088956–01) from the National Institutes of Health.

1. Hannun YA, Obeid LM (2008) Principles of bioactive lipid signalling: Lessons from sphingolipids. *Nat Rev Mol Cell Biol* 9:139–150.
2. Takabe K, Paugh SW, Milstien S, Spiegel S (2008) ''Inside-out'' signaling of sphingosine-1-phosphate: Therapeutic targets. *Pharmacol Rev* 60:181–195.
3. Zhang H, et al. (1991) Sphingosine-1-phosphate, a novel lipid, involved in cellular proliferation. *J Cell Biol* 114:155–167.
4. An S, Goetzl EJ, Lee H (1998) Signaling mechanisms and molecular characteristics of G protein-coupled receptors for lysophosphatidic acid and sphingosine 1-phosphate. *J Cell Biochem Suppl* 30–31:147–157.
5. Maceyka M, Payne SG, Milstien S, Spiegel S (2002) Sphingosine kinase, sphingosine-1-phosphate, and apoptosis. *Biochim Biophys Acta* 1585:193–201.
6. Van Brocklyn JR, et al. (1998) Dual actions of sphingosine-1-phosphate: Extracellular through the Gi-coupled receptor Edg-1 and intracellular to regulate proliferation and survival. *J Cell Biol* 142:229–240.
7. Gardell SE, Dubin AE, Chun J (2006) Emerging medicinal roles for lysophospholipid signaling. *Trends Mol Med* 12:65–75.
8. Visentin B, et al. (2006) Validation of an anti-sphingosine-1-phosphate antibody as a potential therapeutic in reducing growth, invasion, and angiogenesis in multiple tumor lineages. *Cancer Cell* 9:225–238.
9. O'Brien N, et al. (June 9, 2009) Production and characterization of monoclonal anti-sphingosine-1-phosphate antibodies. *J Lipid Res*, 10.1194/jlr.M900048-JLR200.
10. Kabat EA, et al. (1991) *Sequences of Proteins of Immunological Interest* (National Institutes of Health, Bethesda, MD), 5th Ed.
11. Tsodikov OV, Record MT, Jr, Sergeev YV (2002) Novel computer program for fast exact calculation of accessible and molecular surface areas and average surface curvature. *J Comput Chem* 23:600–609.
12. Pozharski E, et al. (2005) Diversity in hapten recognition: Structural study of an anti-cocaine antibody M82G2. *J Mol Biol* 349:570–582.
13. Viadiu H, Aggarwal AK (1998) The role of metals in catalysis by the restriction endonuclease BamHI. *Nat Struct Biol* 5:910–916.
14. Horton JR, Cheng X (2000) PvuII endonuclease contains two calcium ions in active sites. *J Mol Biol* 300:1049–1056.
15. Swairjo MA, et al. (1995) $Ca^{2+}$-bridging mechanism and phospholipid head group recognition in the membrane-binding protein annexin V. *Nat Struct Biol* 2:968–974.
16. Verdaguer N, et al. (1999) $Ca^{2+}$ bridges the C2 membrane-binding domain of protein kinase Calpha directly to phosphatidylserine. *EMBO J* 18:6329–6338.
17. Huang M, et al. (2003) Structural basis of membrane binding by Gla domains of vitamin K-dependent proteins. *Nat Struct Biol* 10:751–756.
18. Roberts VA, Getzoff ED (1995) Metalloantibody design. *FASEB J* 9:94–100.
19. Trisler K, et al. (2007) A metalloantibody that irreversibly binds a protein antigen. *J Biol Chem* 282:26344–26353.
20. Zhou T, et al. (2005) Interfacial metal and antibody recognition. *Proc Natl Acad Sci USA* 102:14575–14580.
21. Landry RC, et al. (2001) Antibody recognition of a conformational epitope in a peptide antigen: Fv-peptide complex of an antibody fragment specific for the mutant EGF receptor, EGFRvIII. *J Mol Biol* 308:883–893.
22. Otwinowski Z, Minor W (1997) in *Macromolecular Crystallography, Part A*, eds Carter, CW, Jr, Sweet, RM (Academic, New York), pp 307–326.
23. McCoy AJ, et al. (2007) Phaser crystallographic software. *J Appl Crystallogr* 40:658–674.
24. Murshudov GN, Vagin AA, Dodson EJ (1997) Refinement of macromolecular structures by the maximum-likelihood method. *Acta Crystallogr D* 53:240–255.
25. McRee DE (1999) XtalView/Xfit—A versatile program for manipulating atomic coordinates and electron density. *J Struct Biol* 125:156–165.
26. Kleywegt GJ, Jones TA (1998) Databases in protein crystallography. *Acta Crystallogr D* 54:1119–1131.
27. Davis IW, et al. (2007) MolProbity: All-atom contacts and structure validation for proteins and nucleic acids. *Nucleic Acids Res* 35:W375–W383.
28. Berman HM, et al. (2000) The Protein Data Bank. *Nucleic Acids Res* 28:235–242.
29. DeLano WL (2008) The PyMOL Molecular Graphics System. (DeLano Scientific LLC, Palo Alto, CA).